JCTC Journal of Chemical Theory and Computation

pubs.acs.org/JCTC Article

Thermochemistry of $FeO_mH_n^z$ Species: Assessment of Some DFT Functionals

Marc Reimann, Florian A. Bischoff, and Joachim Sauer*

Cite This: J. Chem. Theory Comput. 2020, 16, 2430−2435 Read Online

ACCESS | Metrics & More | Article Recommendations | Supporting Information

ABSTRACT: Thermochemical data for 20 anionic, cationic, and neutral gas-phase species, including $Fe^{0/+}$, $FeO^{-/0/+/2+}$, $FeOH^{0/+/2+}$, $FeO_2^{-/0/+}$, $OFeOH^{0/+}$, $Fe(OH)_2^{0/+}$, $Fe(H_2O)^{+/2+}$, and $Fe(H_2O)_2^{+/2+}$ with oxidation states between +I and +IV for Fe and −I and −II for O, compiled by Schröder [*J. Phys. Chem. A* **2008**, *112*, 13215], are used to assess the performance of the "Jacob's ladder" functionals PBE, TPSS, PBE0, and TPSSh for the SVP, TZVP, and QZVP basis sets. In addition, the BP86 and B3LYP functionals are considered. The TPSSh functional performs best. With the TZVP basis set (recommended), the mean absolute and the maximum errors are 24 and 63 kJ/mol, respectively. With 32 and 78 kJ/mol, respectively, BP86 is second best, better than PBE.

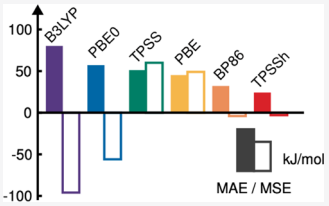

INTRODUCTION

Iron oxo-hydroxo compounds are ubiquitous in the earth's crust, involved in industrial applications, and essential for biological processes. They occur as minerals, synthetic materials such as solid (earth-abundant) catalysts, and also as enzymes and numerous bioinspired and biomimetic inorganic compounds.[1−4]

Atomistic understanding of these complex compounds cannot be gained without quantum chemical calculations, which are challenging not only because of the size of relevant models but also because of the complex electronic structure of Fe compounds with partially occupied d-shells and many possible electron configurations and spin states. When density functional theory (DFT) is applied, the choice of the functional becomes crucial. For comparative tests of density functionals, we need to know the right answer for a test set of systems, either from experiment or from wave-function-based calculations; see, e.g., ref 5. The wave function calculations are limited to small systems, mostly diatomics,[6,7] and, even for triatomics with one Fe atom, difficult to converge with respect to the active space, the dynamical correlation treatment, and the one-particle basis set; see, e.g., a study on FeO_2^+.[8]

For iron-oxo-hydroxy compounds, $FeO_mH_n^z$, "gaseous rust", Schröder[9] compiled standard enthalpies of formation for 24 anionic, cationic, and neutral gas-phase species, including $Fe^{0/+}$, $FeO^{-/0/+/2+}$, $FeOH^{0/+/2+}$, $FeO_2^{-/0/+}$, $OFeOH^{0/+}$, $Fe(OH)_2^{-/0/+/2+}$, $Fe(H_2O)^{+/2+}$, $(H_2O)FeOH^{+/2+}$, and $Fe(H_2O)_2^{+/2+}$. Experimental and theoretical values were refined through a thermochemical network.[9] Since the determination of individual thermochemical quantities might exhibit large and ill-defined errors, the network approach can reveal outliers and thus give heats of formation of consistent quality for all species. This feature renders thermochemical networks, see, e.g., also ref 10, suitable for being the reference in assessment studies. As we will show below, the oxidation states vary widely in this set of $FeO_mH_n^z$ species, +I, +II, +III, and +IV for Fe and −I and −II for O, which adds to its attractiveness for testing functionals.

We are looking for functionals that are suitable for use, for example, in global structure optimizations of multinuclear iron oxo-hydroxo compounds in the gas phase with the aim to assign their vibrational spectra, similar to the recent study on $[Al_3O_4(D_2O)_{1-4}]^+$.[11] As Schröder's gaseous rust,[9] the Fe-substituted clusters will serve as experimental model systems for the complex oxide structures studied in heterogeneous catalysis.[12] Another topical area of application is computational studies of the interaction of water with iron oxide surfaces.[13−16]

Here, we will use the well-defined thermochemical data set for iron oxo-hydroxy compounds[9] to assess the performance of the "Jacob's ladder" series[17] of functionals: PBE[18−20]−TPSS[21]−PBE0[22]−TPSSh.[23] In addition, we test the widely used BP86[24,25] and B3LYP[26] functionals. We do not include functionals with a higher amount of Fock exchange because published tests for 3d transition metal compounds[5,27] and our own results indicate that this worsens the agreement.

Since the values given for $Fe(OH)_2^{-/2+}$ and (H_2O)-$FeOH^{+/2+}$ are not fully derived from the experiment but include calculated B3LYP values, we exclude these four species from our considerations. All statistical values shown below correspond to the test set of 20 species, and the results for all 24 species are given in the Supporting Information.

Received: January 26, 2020
Published: March 27, 2020

https://dx.doi.org/10.1021/acs.jctc.0c00088
J. Chem. Theory Comput. 2020, 16, 2430−2435

Table 1. Standard Enthalpies of Formation at 0 K (kJ/mol) Obtained with the TZVP Basis Set and Various Density Functionals

	exp.[9]	PBE	TPSS	PBE0	TPSSh	BP86	B3LYP
Fe	413 ± 1.3	322	474	478	400	(413)[b]	279
Fe^+	1176 ± 1.3	1054	1234	1213	1119	1185	1021
FeO^-	108 ± 6	156	175	90	128	88	24
FeO	252 ± 6	253	260	180	210	195	126
FeO^+	1088 ± 6	1098	1104	1003	1044	1055	960
FeO^{2+}	2795 ± 28	2895	2882	2804	2826	2864	2767
FeOH	129 ± 15	198	210	31	122	144	10
$FeOH^+$	870 ± 15	899	904	746	821	858	719
$FeOH^{2+}$	2447 ± 30	2505	2504	2361	2424	2477	2338
FeO_2^-	−161 ± 13	−120	−111	−136	−137	−190	−211
FeO_2	67 ± 12	68	86	89	73	14	15
FeO_2^+	1062 ± 25	1053	1068	1134	1078	1014	1052
OFeOH	−84 ± 17	−44	−27	−124	−68	−97	−166
$OFeOH^+$	852 ± 23	816	837	802	809	778	747
$Fe(OH)_2^-$[a]	−431	−299	−268	−423	−341	−360	−466
$Fe(OH)_2$	−322 ± 2	−196	−175	−351	−259	−247	−378
$Fe(OH)_2^+$	561 ± 10	636	662	514	590	600	488
$Fe(OH)_2^{2+}$[a]	2252	2234	2258	2201	2223	2211	2157
$Fe(H_2O)^+$	809 ± 5	852	861	680	768	813	650
$Fe(H_2O)^{2+}$	2129 ± 29	2232	2235	2019	2128	2207	2017
$(H_2O)FeOH^+$[a]	405	493	522	326	432	457	310
$(H_2O)FeOH^{2+}$[a]	1864	1942	1971	1794	1888	1920	1782
$Fe(H_2O)_2^+$	406 ± 6	467	510	296	415	437	277
$Fe(H_2O)_2^{2+}$	1570 ± 29	1693	1725	1479	1614	1674	1484

[a]The experimental values for these species include calculated values. They are therefore excluded from the statistical evaluation. [b]The atomization energy of Fe could not be calculated for the BP86 functional and is therefore taken as the experimental value.

Tests on transition metal compounds, including species considered here, have been performed before. The B3LYP functional[26] was employed by Gutsev et al. in early studies of 3d metal monoxides and dioxides.[28,29] Furche and Perdew tested semilocal and hybrid density functionals for 3d transition metal compounds, mostly diatomics,[30] among them were also FeH and FeO, and found TPSSh to perform best for thermochemistry. In agreement with that, Jensen[31,32] and Reiher[33] found TPSSh and PBE0 superior to other functionals. Truhlar et al. investigated the performance of 42 different exchange−correlation functionals, including most examined here, for their 3dBE70 database of bond dissociation energies of 70 small molecules and showed that TPSSh shows the smallest mean-signed error (MSE), and, together with other hybrid meta GGA functionals (GGA − generalized gradient approximation), belongs to the best performing functionals.[27]

METHODS

Computational Details. All calculations except those on the Fe metal were performed with the Turbomole program.[34] The following "Ahlrichs" basis sets,[35] labeled "def2" in the Turbomole library, were used: SVP (Fe: 5s3p2d1f, O: 3s2p1d, H: 2s1p), TZVP (Fe: 6s4p4d1f, O: 5s3p2d1f, H: 3s1p), and QZVP (Fe: 11s6p5d3f1g, O: 7s4p3d2f1g, H: 4s3p2d1f). Standard quadrature grids with 434 spherical grid points (grid size 4) were employed.[36] These are sufficient even for the considered anionic species FeO^-, FeO_2^-, and $Fe(OH)_2^-$ (see the Supporting Information, Table S7), for which also additional basis sets with more diffuse functions[37] have been used. The calculated ionization energies show that extension beyond QZVP changes the results by 1−3 kJ/mol only.

For the anions, the highest occupied orbital has positive energies for all basis sets and all functionals considered, with the exception of FeO_2^- with PBE0/TZVP, PBE0/QZVP, and B3LYP/QZVP. However, the anions are always more stable (lower total energy) than the corresponding neutral systems; see also the ionization energies in Table S7 of the Supporting Information.

Calculations were performed in C_1-symmetry and the structure optimizations used internal coordinates. Convergence criteria were chosen to be 0.1 μE_H for total energies and 1 mE_H/a_0 for gradients. Harmonic vibrational frequencies were used to compute thermal corrections. All calculations were performed using unrestricted reference functions. The spin state of the different species was chosen by comparative calculation of different possible spin states and using the spin state of lowest energy.

Constructing broken symmetry solutions as recently described by Radoń[38] did not lead to lower energy solutions for any system using a TZVP basis set and either the BP86 or the TPSSh functional.

The atomization energy of the Fe metal was computed with a local version of the VASP program[39] modified to include the TPSSh functional.

Heats of Formation. The experimentally accessible standard reaction enthalpies $\Delta_r H^\circ$

$$\nu_1 X_1 + \nu_2 X_2 + \ldots \rightarrow \nu_Z Z \tag{1}$$

can be computed from the heats of formation $\Delta_f H_i^\circ$ of the components

$$\Delta_r H^\circ = \sum_{i=1}^{Z} \nu_i \, \Delta_f H_i^\circ \tag{2}$$

https://dx.doi.org/10.1021/acs.jctc.0c00088
J. Chem. Theory Comput. 2020, 16, 2430−2435

The latter are computed from the energies of formation $\Delta_f E$ of all involved species (the atomization energies), the zero-point vibrational energies, ΔE_{ZPV}, and thermal corrections, ΔH_T

$$\Delta_f H^\circ_{298} = \Delta_f E + \Delta E_{ZPV} + \Delta H_T = \Delta_f H^\circ_0 + \Delta H_T \quad (3)$$

As already noted by Kellogg and Irikura,[40] the thermal corrections turn out be small, significantly smaller (<9 kJ/mol; see the Supporting Information) than the deviations between DFT and the experiment. The reference values are also heats of formation at 0 K because "temperatures are not unequivocally defined in all experiments".[9]

Statistics. Comparison of the DFT results to the reference values is made using the usual statistical measures. Defining x_i as the difference between the calculated value $x_{i,calc}$ and the reference value $x_{i,ref}$, we obtain the mean signed and mean absolute errors, MSE and MAE, respectively, as well as the standard deviation, σ, as

$$\mathrm{MSE} = \frac{1}{N}\sum_{i=1}^{N} x_i = \bar{x}$$

$$\mathrm{MAE} = \frac{1}{N}\sum_{i=1}^{N} |x_i|$$

$$\sigma = \sqrt{\frac{1}{N}\sum_{i=1}^{N} (x_i - \bar{x})^2}$$

Since we are primarily interested in global structure optimizations, we consider the standard deviation most relevant, whereas mean errors only show an offset of all energies. We also provide root mean square errors (RMSE) that can be obtained from the mean signed error and the standard deviation

$$\mathrm{RMSE}^2 = \frac{1}{N}\sum_{i=1}^{N} x_i^2 = \mathrm{MSE}^2 + \sigma^2$$

Only in part, the reference values[9] are directly measured, others are taken from a thermochemical network. As such, they have standard deviations attributed to them. One possible way to take experimental uncertainties δ_i of the reference values into account is by defining a corrected RMSE, cRMSE

$$\mathrm{cRMSE}^2 = \frac{1}{N}\sum_{i=1}^{N} (x_i^2 + \delta_i^2) \geq \mathrm{RMSE}^2$$

In our case, the difference between the RMSE and the cRMSE value is between 1 and 3 kJ/mol, which changes the RMSE value by less than 5% (10% for the TPSSh functional that has very small RMSE values), see the Supporting Information (Table S2), and, hence, can safely be neglected.

RESULTS

Table 1 shows the standard enthalpies of formation obtained with the TZVP basis set for all functionals considered and Table 2 the statistical measures for the comparison with the test set of 20 species. For comparison with the full set of 24 species, see the Supporting Information, Table S3. The atomization enthalpies of Fe, O, and H are also calculated with the respective density functional (except for BP86) and shown in Table S6. Sometimes the atomization energies of elements are taken from the experiment. For the statistical measures for all functionals using experimental atomization energies for Fe, O, and H, see the Supporting Information, Table S5.

Table 2. Statistical Measures for the Standard Enthalpies of Formation at 0 K Obtained with Various Density Functionals and the TZVP and QZVP Basis Sets (kJ/mol)

TZVP	PBE	TPSS	PBE0	TPSSh	BP86	B3LYP
MAE	45	51	57	24	32	80
MSE	49	60	−56	−3	4	−95
maximum error	126	147	−129	63	78	−159
standard deviation	40	42	54	33	45	41
RMSE	64	73	78	33	46	104
QZVP	PBE	TPSS	PBE0	TPSSh	BP86	B3LYP
MAE	36	40	65	23	34	90
MSE	33	43	−74	−20	−11	−108
maximum error	101	122	−139	−62	−88	−163
standard deviation	41	40	48	29	47	38
RMSE	52	59	88	35	48	114

We focus here on the "(def2)" TZVP basis sets,[35] which includes f-functions on Fe and O because this is the most likely choice in applications. While Table 2 also includes statistical measures for the largest basis set studied, QZVP, those for the smaller SVP basis set are given in the Supporting Information.

For the TZVP basis set, the TPSSh functional performs best. The standard deviation is 33 kJ/mol and the mean absolute (MAE) and mean signed errors (MSE) are 24 and −3 kJ/mol, respectively, whereas the maximum error is as large as 63 kJ/mol. The PBE functional is clearly inferior, but it is remarkable that neither the TPSS meta-GGA nor the PBE0 hybrid functional are an improvement compared to PBE. On inclusion of Fock exchange, when passing from PBE to PBE0, the MAE increases from 45 to 57 kJ/mol, whereas the MSE and the maximum error change the sign from 49 to −56 kJ/mol and from 126 to −129 kJ/mol, respectively. Comparison of the B3LYP hybrid functional with the BP86 functional shows a similar pattern. The result of this comparison is not unexpected[41] as the performance of DFT functionals in transition metal compounds typically depends strongly on the amount of Fock exchange.

For B3LYP, PBE, TPSS, and PBE0, MAE and MSE agree, except for the sign, within 15, 4, 1, and 1 kJ/mol, respectively, indicating that the deviations, although large, are pretty systematic. Whereas PBE and TPSS overestimate the enthalpies of formation by 49 and 60 kJ/mol, respectively, PBE0 and B3LYP underestimate them by 56 and 95 kJ/mol, respectively.

For the larger QZVP basis set, the same observations are made as for TZVP when comparing the different functionals; see Table 2. The MAEs are smaller for PBE and TPSS, larger for the hybrid functionals PBE0 and B3LYP, and about the same for TPSSh and BP86. For the best performing TPSSh functional, passing to the more diffuse QZVP basis sets improves the description of the anionic systems as expected, and the calculated ionization energies get closer to the experiment (by 29 and 18 kJ/mol for FeO^- and FeO_2^-, respectively; see Table S7). However, this does not improve the overall performance, except that the deviations become more systematic: from TZVP to QZVP the MAE changes from 24 to 23 kJ/mol and the MSE from −3 to −20 kJ/mol.

The use of the SVP basis set increases the standard deviations and the MSEs for all functionals significantly, but

https://dx.doi.org/10.1021/acs.jctc.0c00088
J. Chem. Theory Comput. 2020, 16, 2430−2435

Table 3. Spin States and Formal Electron Configurations (Form. El. Conf.) of Fe for All Species with TPSSh/QZVP[a]

	natural orbital population						oxidation state	
species	4s	3d	total	$\langle S^2\rangle$	valence state	$\langle S^2\rangle_{\text{theor.}}$	Fe	O
Fe	1.38	6.61	7.99	6.01	Fe	6.00	0	
Fe^+	0.00	7.00	7.00	3.75	Fe^+	3.75[b]	+I	
FeO^-	1.32	6.45	7.77	4.13	$Fe-O^-$	3.75	+I	−II
FeO	0.52	6.56	7.08	6.03	Fe^+-O^-	6.00	+II	−II
					$Fe^+[O^{\bullet -}]$		+I	−I
FeO^+	0.24	6.24	6.48	8.76	$Fe^{2+}-O^-$	8.75	+III	−II
					$Fe^+-O^\bullet$		+II	−I
FeO^{2+}	0.00	6.02	6.02	6.23	$Fe^{2+}-O^\bullet$	6.00	+III	−I
FeOH	0.94	6.24	7.18	8.75	Fe^+OH^-	8.75	+I	−II
$FeOH^+$	0.12	6.39	6.51	6.01	$Fe^{2+}OH^-$	6.00	+II	−II
$FeOH^{2+}$	0.04	5.97	6.01	8.76	$Fe^{2+}[^\bullet OH]$	8.75	+II	−I
FeO_2^-	0.43	6.47	6.90	3.82	$O^--Fe^+-O^-$	3.75	+III	−II/−II
					$O^--Fe^{+\bullet}O^-$		+II	−II/−I
FeO_2	0.34	6.29	6.63	6.05	$O^--Fe^+-O^\bullet$	6.00	+III	−II/−I
					$O^--Fe^{2+\bullet}O^-$			
FeO_2^+	0.11	6.37	6.48	3.81	$^\bullet O-Fe^+-O^\bullet$	3.75	+III	−I/−I
					$^\bullet O-Fe^{2+}-O^-$		+IV	−I/−II
OFeOH	0.32	6.39	6.71	3.85	$^\bullet O-Fe^+OH^-$	3.75[c]		
$OFeOH^+$	0.18	6.21	6.39	6.05	$^\bullet O-Fe^{2+}OH^-$	6.00	+III	−I/−II
$Fe(OH)_2^-$	0.98	6.48	7.46	3.87	$HO-Fe(OH^-)$	3.75	+I	−II/−II
					$Fe^+(OH^-)_2$			
$Fe(OH)_2$	0.30	6.32	6.62	6.01	$HO-Fe^+(OH^-)$	6.00	+IV	−II/−II
					$Fe^{2+}(OH^-)_2$			
$Fe(OH)_2^+$	0.18	5.97	6.15	8.76	$HO-Fe^{2+}(OH^-)$	8.75	+III	−II/−II
$Fe(OH)_2^{2+}$	0.11	5.99	6.10	6.10	$HO-Fe^{2+}-OH$	6.00	+IV	−II
$Fe(H_2O)^+$	0.12	6.93	7.05	3.75	$Fe^+(H_2O)$	3.75	+I	(−II)
$Fe(H_2O)^{2+}$	0.04	6.13	6.17	6.00	$Fe^{2+}(H_2O)$	6.00	+II	(−II)
$(H_2O)FeOH^+$	0.21	6.34	6.55	6.01	$(H_2O)Fe^{2+}OH^-$	6.00	+II	−II
$(H_2O)FeOH^{2+}$	0.16	5.90	6.06	8.76	$(H_2O)Fe^{2+\bullet}OH$	8.75	+II	
$Fe(H_2O)_2^+$	0.56	6.63	7.19	3.78	$Fe^+(H_2O)_2$	3.75	+I	
$Fe(H_2O)_2^{2+}$	0.14	6.14	6.28	6.00	$Fe^{2+}(H_2O)_2$	6.00	+II	

[a]Natural orbital configurations were taken from a Natural Population Analysis (NPA). [b]All functionals except for TPSS predict a $\langle S^2\rangle_{\text{theor.}}$ = 8.75, 4s(1) 3d(6) high spin configuration for SVP basis set. [c]For B3LYP and PBE0, the most stable spin state is the $\langle S^2\rangle_{\text{theor}}$ = 8.75.

TPSSh still performs best. For TPSSh, MAE and maximum errors are 35 and 81 kJ/mol, respectively, whereas, for PBE, they are 83 and −205 kJ/mol, respectively.

Table 3 shows the spin states, $\langle S^2\rangle = S(S+1)$ obtained in this work for the TPSSh functional and the QZVP basis set. In some cases, e.g., Fe^+ and OFeOH, the functionals disagree on the most stable spin state of the molecules. For Fe^+, the spin state also depends on the basis set: sextet for SVP but quartet for TZVP and QZVP. Only the TPSS functional yields a quartet with all the basis sets studied. Experimentally, the quartet excited state is 22.4 kJ/mol higher in energy than the sextet ground state.[42]

Table 3 also shows the natural orbital populations[43] of the Fe 4s and 3d states. From the latter and the spin state, electron configurations and valence states can be derived, which we also show in Table 3. Sometimes 4s and 3d populations together with the spin are compatible with two different valence states with different oxidation states of Fe and O.

Let us consider FeO as an example. There are seven electrons on Fe, which means that Fe has given one electron to O and becomes Fe^+ and O becomes O^-. The occupation of the 4s with about half an electron suggests that two electron configurations may play a role with either one or no electron occupying the 4s orbital. In the former case, there are six electrons in 3d orbitals, which leaves four unpaired electrons in d states. One couples with the unpaired electron on the $O^{\bullet -}$, which leaves four unpaired spins, one in 4s and three in 3d. The total spin of two yields $\langle S^2\rangle$ = 6, which explains the calculated value of 6.03. The oxidation state of Fe is +II and of O −II (one electron transferred and one bond formed). If there is no electron in the 4s orbital, there remain three unpaired electrons in 3d states. A ferromagnetic coupling of these spins with spin on $O^{\bullet -}$ would also yield S = 2, but the oxidation state may rather be considered +I and −I for Fe and O, respectively.

DISCUSSION

Our results are in line with other comparative studies on different density functionals for transition metal chemistry. Furche and Perdew[30] also reached the conclusion that TPSSh performs best for bond dissociation energies and thermochemistry, with an MAE of 33 kJ/mol for reaction energies in a QZVP basis. For this basis set, we get a mean absolute error of 23 kJ/mol (Table 2) in very good agreement. They also found B3LYP to show "a rather erratic behavior" with an MAE of 54 kJ/mol.[30] The large MAE of 90 kJ/mol for the B3LYP functional in the present work is due to its bad performance for solid iron. When experimental values are used for the elements

https://dx.doi.org/10.1021/acs.jctc.0c00088
J. Chem. Theory Comput. 2020, 16, 2430−2435

instead, the MAE is 30 kJ/mol (Supporting information, Table S5).

Comparison of the TZVP results in Table S5 with a set of 60 diatomics of d-block metals[5] shows a better performance of the meta-GGA functionals with our iron oxo-hydroxo compounds (MAEs decrease from 57 to 29, 42 to 30, and 52 to 34 for PBE, TPSS, and BP86, respectively) but a worse performance for hybrid functionals (MAEs increase from 25 to 42 and 24 to 40 for PBE0 and B3LYP, respectively).

Chen, Reiher, and co-workers studied various large cationic transition metal complexes and used 10 ligand dissociation energies to assess different functionals.[33] They concluded: "PBE0 and TPSSh are the two most accurate functionals for our test set, but also these functionals exhibit deviations from experimental results by up to 50 kJ/mol for individual reactions".[33] This fits to the maximum errors of 63 and −62 kJ/mol that we find for TPSSh with the TZVP and QZVP basis sets, respectively.

For the relative energies of the electronic states of different isomers of FeO_2^+, compared to multireference calculations, TPSSh performed similar to TPSS and PBE: all showed mean absolute deviations between 17 and 23 kJ/mol using Ahlrichs' TZVPP basis set.[8] For FeO, our result is in perfect agreement with that of Jensen et al.[31] except for the overall better performance of PBE0 (RMSE = 42 kJ/mol, here 78 kJ/mol).[31] With an RMSE of 34 kJ/mol, the TPSSh functional is also found to be superior to all assessed functionals.[32] Our overall RMSE of 33 kJ/mol is in perfect agreement with that as well.

For their 3dBE70 database of bond dissociation energies of 70 small molecules containing a single 3d metal atom, Truhlar and co-workers showed that TPSSh gives the best MSE over the whole set of functionals (1 kJ/mol) and a very good MAE of 18 kJ/mol.[27] Taking into account that these errors are given per bond, this is again in very good agreement with the present results of 14 and 26 kJ/mol, respectively, obtained with experimental values for solid-state Fe (Supporting Information, Table S5, the 3dBE70 set does not include solids).

CONCLUSIONS

In agreement with previous studies,[27,30,32,44] we found the TPSSh functional, the fourth rung of the Jacob's ladder and the highest among those considered here,[17] to perform best with mean absolute errors of 24 and 23 kJ/mol using TZVP and QZVP basis sets, respectively. For PBE, the mean absolute errors are much larger, 45 and 36 kJ/mol, respectively, whereas BP86 performs second best with mean absolute errors of 32 and 34 kJ/mol, respectively. For the same basis set, the change from the generalized gradient approximation functional PBE to TPSSh increases the average calculation time by a factor of about 2. Increasing the basis set from TZVP to QZVP increases the average calculation time by a factor of about 8 while decreasing the standard deviation by only up to 6 kJ/mol. We thus recommend the use of TPSSh with the TZVP basis set for iron oxo-hydroxo compounds.

ASSOCIATED CONTENT

Supporting Information

The Supporting Information is available free of charge at https://pubs.acs.org/doi/10.1021/acs.jctc.0c00088.

Vibrational contributions to enthalpies, additional results for statistical measures obtained with SVP and QZVP basis sets as well as with experimental atomization energies for the elements (Fe, O, H) (PDF)

AUTHOR INFORMATION

Corresponding Author

Joachim Sauer − *Institut für Chemie, Humboldt-Universität zu Berlin D-10099 Berlin, Germany;* orcid.org/0000-0001-6798-6212; Email: js@chemie.hu-berlin.de

Authors

Marc Reimann − *Institut für Chemie, Humboldt-Universität zu Berlin D-10099 Berlin, Germany*

Florian A. Bischoff − *Institut für Chemie, Humboldt-Universität zu Berlin D-10099 Berlin, Germany;* orcid.org/0000-0002-7717-3183

Complete contact information is available at: https://pubs.acs.org/10.1021/acs.jctc.0c00088

Notes

The authors declare no competing financial interest.

ACKNOWLEDGMENTS

This work has been funded by the Deutsche Forschungsgemeinschaft (DFG, German Research Foundation), project 430942176, and supported by the "Fonds der Chemischen Industrie". We thank Dr. Joachim Paier, Berlin, for the implementation of the TPSSh functional into VASP and for assistance with the plane-wave calculations.

REFERENCES

(1) Chen, Z.; Yin, G. The reactivity of the active metal oxo and hydroxo intermediates and their implications in oxidations. *Chem. Soc. Rev.* **2015**, *44*, 1083−1100.

(2) Engelmann, X.; Monte-Perez, I.; Ray, K. Oxidation Reactions with Bioinspired Mononuclear Non-Heme Metal-Oxo Complexes. *Angew. Chem., Int. Ed.* **2016**, *55*, 7632−7649.

(3) Olivo, G.; Cusso, O.; Borrell, M.; Costas, M. Oxidation of alkane and alkene moieties with biologically inspired nonheme iron catalysts and hydrogen peroxide: from free radicals to stereoselective transformations. *J. Biol. Inorg. Chem.* **2017**, *22*, 425−452.

(4) Snyder, B. E. R.; Bols, M. L.; Schoonheydt, R. A.; Sels, B. F.; Solomon, E. I. Iron and Copper Active Sites in Zeolites and Their Correlation to Metalloenzymes. *Chem. Rev.* **2018**, *118*, 2718−2768.

(5) Aoto, Y. A.; de Lima Batista, A. P.; Köhn, A.; de Oliveira-Filho, A. G. S. How To Arrive at Accurate Benchmark Values for Transition Metal Compounds: Computation or Experiment? *J. Chem. Theory Comput.* **2017**, *13*, 5291−5316.

(6) Hait, D.; Tubman, N. M.; Levine, D. S.; Whaley, K. B.; Head-Gordon, M. What Levels of Coupled Cluster Theory Are Appropriate for Transition Metal Systems? A Study Using Near-Exact Quantum Chemical Values for 3d Transition Metal Binary Compounds. *J. Chem. Theory Comput.* **2019**, *15*, 5370−5385.

(7) Shee, J.; Rudshteyn, B.; Arthur, E. J.; Zhang, S.; Reichman, D. R.; Friesner, R. A. On Achieving High Accuracy in Quantum Chemical Calculations of 3d Transition Metal-Containing Systems: A Comparison of Auxiliary-Field Quantum Monte Carlo with Coupled Cluster, Density Functional Theory, and Experiment for Diatomic Molecules. *J. Chem. Theory Comput.* **2019**, *15*, 2346−2358.

(8) Maier, T. M.; Boese, A. D.; Sauer, J.; Wende, T.; Fagiani, M.; Asmis, K. R. The vibrational spectrum of FeO2+ isomers—Theoretical benchmark and experiment. *J. Chem. Phys.* **2014**, *140*, No. 204315.

(9) Schröder, D. Gaseous rust: thermochemistry of neutral and ionic iron oxides and hydroxides in the gas phase. *J. Phys. Chem. A* **2008**, *112*, 13215−13224.

(10) Schröder, D.; Bärsch, S.; Schwarz, H. Second ionization energies of gaseous iron oxides and hydroxides: The FeOmHn2+ dications (m = 1, 2; n < = 4). *J. Phys. Chem. A* **2000**, *104*, 5101−5110.
(11) Fagiani, M. R.; Song, X.; Debnath, S.; Gewinner, S.; Schollkopf, W.; Asmis, K. R.; Bischoff, F. A.; Muller, F.; Sauer, J. Dissociative Water Adsorption by Al3O4+ in the Gas Phase. *J. Phys. Chem. Lett.* **2017**, *8*, 1272−1277.
(12) Sauer, J.; Freund, H.-J. Models in Catalysis. *Catal. Lett.* **2015**, *145*, 109−125.
(13) Kendelewicz, T.; Kaya, S.; Newberg, J. T.; Bluhm, H.; Mulakaluri, N.; Moritz, W.; Scheffler, M.; Nilsson, A.; Pentcheva, R.; Brown, G. E., Jr. X-Ray Photoemission and Density Functional Theory Study of the Interaction of Water Vapor with the Fe3O4(001) Surface at Near-Ambient Conditions. *J. Phys. Chem. C* **2013**, *117*, 2719−2733.
(14) Mirabella, F.; Zaki, E.; Ivars-Barceló, F.; Li, X.; Paier, J.; Sauer, J.; Shaikhutdinov, S.; Freund, H.-J. Cooperative formation of long-range ordering in water ad-layers on Fe3O4(111). *Angew. Chem., Int. Ed.* **2018**, *57*, 1409−1413.
(15) Zaki, E.; Mirabella, F.; Ivars-Barceló, F.; Seifert, J.; Carey, S.; Shaikhutdinov, S.; Freund, H.-J.; Li, X.; Paier, J.; Sauer, J. Water adsorption on the Fe3O4(111) surface: dissociation and network formation. *Phys. Chem. Chem. Phys.* **2018**, *20*, 15764−15774.
(16) Schöttner, L.; Ovcharenko, R.; Nefedov, A.; Voloshina, E.; Wang, Y.; Sauer, J.; Wöll, C. Interaction of Water Molecules with the a-Fe2O3 (0001) Surface: A Combined Experimental and Computational Study. *J. Phys. Chem. C* **2019**, *123*, 8324−8335.
(17) Perdew, J. P.; Schmidt, K. In *Jacob's Ladder of Density Functional Approximations for the Exchange-Correlation Energy*, AIP Conference Proceedings, 2001; Vol. *57*, p 1.
(18) Perdew, J. P.; Burke, K.; Ernzerhof, M. Generalized gradient approximation made simple. *Phys. Rev. Lett.* **1996**, *77*, 3865−3868.
(19) Perdew, J. P.; Burke, K.; Ernzerhof, M. Generalized gradient approximation made simple. *Phys. Rev. Lett.* **1997**, *78*, 1396.
(20) Becke, A. D. Density-Functional Exchange-Energy Approximation with Correct Asymptotic-Behavior. *Phys. Rev. A* **1988**, *38*, 3098−3100.
(21) Tao, J. M.; Perdew, J. P.; Staroverov, V. N.; Scuseria, G. E. Climbing the density functional ladder: Nonempirical meta-generalized gradient approximation designed for molecules and solids. *Phys. Rev. Lett.* **2003**, *91*, No. 146401.
(22) Adamo, C.; Barone, V. Toward reliable density functional methods without adjustable parameters: The PBE0 model. *J. Chem. Phys.* **1999**, *110*, 6158−6170.
(23) Staroverov, V. N.; Scuseria, G. E.; Tao, J. M.; Perdew, J. P. Comparative assessment of a new nonempirical density functional: Molecules and hydrogen-bonded complexes. *J. Chem. Phys.* **2003**, *119*, 12129−12137.
(24) Perdew, J. P. Density-Functional Approximation for the Correlation-Energy of the Inhomogeneous Electron-Gas. *Phys. Rev. B* **1986**, *33*, 8822−8824.
(25) Perdew, J. P. Correction. *Phys. Rev. B* **1986**, *34*, 7406.
(26) Becke, A. D. Density-Functional Thermochemistry 3. The Role of Exact Exchange. *J. Chem. Phys.* **1993**, *98*, 5648−5652.
(27) Zhang, W.; Truhlar, D. G.; Tang, M. Tests of Exchange-Correlation Functional Approximations Against Reliable Experimental Data for Average Bond Energies of 3d Transition Metal Compounds. *J. Chem. Theory Comput.* **2013**, *9*, 3965−3977.
(28) Gutsev, G. L.; Rao, B. K.; Jena, P. Electronic Structure of the 3d Metal Monoxide Anions. *J. Phys. Chem. A* **2000**, *104*, 5374−5379.
(29) Gutsev, G. L.; Rao, B. K.; Jena, P. Systematic Study of Oxo, Peroxo, and Superoxo Isomers of 3d-Metal Dioxides and Their Anions. *J. Phys. Chem. A* **2000**, *104*, 11961−11971.
(30) Furche, F.; Perdew, J. P. The performance of semilocal and hybrid density functionals in 3d transition-metal chemistry. *J. Chem. Phys.* **2006**, *124*, No. 044103.
(31) Jensen, K. P.; Roos, B. O.; Ryde, U. Performance of density functionals for first row transition metal systems. *J. Chem. Phys.* **2007**, *126*, No. 014103.
(32) Jensen, K. P. Bioinorganic Chemistry Modeled with the TPSSh Density Functional. *Inorg. Chem.* **2008**, *47*, 10357−10365.
(33) Weymuth, T.; Couzijn, E. P. A.; Chen, P.; Reiher, M. New Benchmark Set of Transition-Metal Coordination Reactions for the Assessment of Density Functionals. *J. Chem. Theory Comput.* **2014**, *10*, 3092−3103.
(34) *TURBOMOLE V6.5 2013, A Development of University of Karlsruhe and Forschungszentrum Karlsruhe GmbH*; TURBOMOLE GmbH, 1989−2007. available from http://www.turbomole.com.
(35) Weigend, F.; Ahlrichs, R. Balanced basis sets of split valence, triple zeta valence and quadruple zeta valence quality for H to Rn: Design and assessment of accuracy. *Phys. Chem. Chem. Phys.* **2005**, *7*, 3297−305.
(36) Treutler, O.; Ahlrichs, R. Efficient Molecular Numerical Integration Schemes. *J. Chem. Phys.* **1995**, *102*, 346−354.
(37) Rappoport, D.; Furche, F. Property-optimized Gaussian basis sets for molecular response calculations. *J. Chem. Phys.* **2010**, *133*, No. 134105.
(38) Radoń, M. Benchmarking quantum chemistry methods for spin-state energetics of iron complexes against quantitative experimental data. *Phys. Chem. Chem. Phys.* **2019**, *21*, 4854−4870.
(39) Kresse, G.; Furthmüller, J. Efficient iterative schemes for ab initio total-energy calculations using a plane-wave basis set. *Phys. Rev. B* **1996**, *54*, 11169−11186.
(40) Kellogg, C. B.; Irikura, K. K. Gas-phase thermochemistry of iron oxides and hydroxides: Portrait of a super-efficient flame suppressant. *J. Phys. Chem. A* **1999**, *103*, 1150−1159.
(41) Rappoport, D.; Crawford, N. R. M.; Furche, F.; Burke, K. Which Functional Should I Use? In *Computational Inorganic and Bioinorganic Chemistry*; Solomon, E. I.; King, R. B.; Scott, R. A., Eds.; Wiley: Chichester, 2008.
(42) Nave, G.; Johansson, S. The Spectrum of Fe II. *Astrophys. J., Suppl. Ser.* **2013**, *204*, 1−8.
(43) Reed, A. E.; Weinstock, R. B.; Weinhold, F. Natural Population Analysis. *J. Chem. Phys.* **1985**, *83*, 735−746.
(44) Schultz, N. E.; Zhao, Y.; Truhlar, D. G. Density functionals for inorganometallic and organometallic chemistry. *J. Phys. Chem. A* **2005**, *109*, 11127−11143.

https://dx.doi.org/10.1021/acs.jctc.0c00088
J. Chem. Theory Comput. 2020, 16, 2430−2435